Electronic Supplementary Material (ESI) for Chemical Science.
This journal is © The Royal Society of Chemistry 2020

In situ visualization of peroxisomal viscosity in the liver of mice with non-alcoholic fatty liver disease by near-infrared fluorescence and photoacoustic imaging

Yongqing Zhou, Ping Li*, Xin Wang, Chuanchen Wu, Nannan Fan, Xiaoning Liu, Lijie Wu, Wei Zhang, Wen Zhang, Zhenzhen Liu and Bo Tang*

College of Chemistry, Chemical Engineering and Materials Science, Key Laboratory of Molecular and Nano Probes, Ministry of Education, Collaborative Innovation Center of Functionalized Probes for Chemical Imaging in Universities of Shandong, Institutes of Biomedical Sciences, Shandong Normal University, Jinan 250014, People's Republic of China.

E-mail: tangb@sdnu.edu.cn, lip@sdnu.edu.cn

Table of Contents

Materials and Instruments

Cell culture

Cell imaging

Mouse models and in vivo liver imaging

Statistical analysis

Fluorescence quantum and the Förster-Hoffmann equation

Scheme S1 Synthesis of PV-1

Table S1. Relative parameters of PV-1 in the methanol/glycerol (v/v) mixtures

Fig. S1 UV spectra and fluorescence spectra of PV-1 in different solvents

Fig. S2 The optimization of PV-1 concentration

Fig. S3 The fit curves of the absorption spectra of PV-1 in methanol-glycerol mixtures

Fig. S4 The fit curves of the absorption spectra and fluorescence spectra of precursor 3 in different solvents and methanol-glycerol mixtures

Fig. S5 The selectivity of the PV-1

Fig. S6 The pH effects on the PV-1

Fig. S7 The photo-stability experiments of PV-1

Fig. S8 The cytotoxicity assay of PV-1

Fig. S9 *In vivo* toxicity of PV-1 in C57 mice

Fig. S10 Confocal fluorescence images of the HL-7702 cells incubated with PV-1

Fig. S11 Time-dependent fluorescence imaging of HL-7702 stained with PV-1

Fig. S12 Weight of normal mice and nonalcoholic fatty liver mice

Fig. S13 The hematoxylin and eosin (H&E) staining of liver in mice

Fig. S14 Fluorescence images of the mouse's liver after the injection of PV-1

Fig. S15 Fluorescence intensity of PV-1 in fresh liver tissue homogenate supernatant under NAC condition

Fig. S16 Fluorescence images of the different organs after the injection of PV-1

Fig. S17 PA_{680nm} images of the mouse's liver after the injection of PV-1

Fig. S18 The relative alanine aminotransferase (ALT) in mice liver

Fig. S19 The ^{1}H NMR, ^{13}C NMR and HRMS data of compound 2

Fig. S20 The ^{1}H NMR, ^{13}C NMR and HRMS data of compound 3

Fig. S21 MS and HPLC data of PV-1

Materials and Instruments

All reagents and solvents were purchased from commercial suppliers and used with not further purification. 3-(4,5-Dimethylthiazol-2-yl)-2,5-diphenyl tetrazolium bromide (MTT) was purchased from Sigma. Peroxisome-GFP, ER-Tracker Red, Lyso-Tracker Green and Mito-Tracker Green were purchased from Invitrogen (U.S.A.). Oleic acid (OA) was purchased from Macklin. Silica gel (200−300 mesh) used for flash column chromatography was purchased from Qingdao Haiyang Chemical Co., Ltd. ^{1}H NMR and ^{13}C NMR spectra were determined at 400 MHz and 100 MHz using Bruker NMR spectrometers. The fluorescence lifetime of the probe PV-1 was measured by Edinburgh FLS1000 Fluorescence Spectrometer. The mass spectra were obtained by a Bruker Maxis ultrahigh-resolution time-of-flight mass spectrometry (TOF MS) system. Viscosity value was recorded by an NDJ-8S rotational viscometer. The MTT assay was performed using a TRITURUS microplate reader. Absorption spectra were recorded on a UV-Vis spectrophotometer (Evolution 220, Thermo Scientific). The fluorescence spectrum measurements were performed using a Hitachi F-4600 fluorescence spectrophotometer (Japan, HITACHI). The co-localized images were recorded on a Leica TCS SP8 microscope with a 63x oil-immersion objective (N/A 1.3). The liver cells HL-7702 cells and SMMC-7721 cells were purchased from the Cell Bank of the Chinese Academy of Sciences (Shanghai, China). In vivo fluorescence imaging of mice was carried out on an in vivo live Imaging system, the Perkinelmer IVIS Spectrum. In vivo photoacoustic imaging of mice was carried out on a photoacoustic tomography system, Endra Nexus 128. Peroxynitrite ($ONOO^-$) was chemically prepared by H_2O_2 and $NaNO_2$, the concentration of it was estimated by using an extinction coefficient of 1670 M^{-1} cm^{-1} (302 nm); $O_2^{\bullet-}$ was prepared by dissolving KO_2 in DMSO solution. Hydroxyl radical (•OH) was produced by the Fenton reaction (Fe^{2+}: H_2O_2 = 1: 10). NO was prepared from sodium nitroprusside. Hydrogen peroxide (H_2O_2), sodium hypochlorite (NaClO) and tert-butyl hydroperoxide (TBHP) were derived from water solutions with contents of 30 %, 10 % and 70 %, respectively. Solutions of metal ions were prepared from chlorizated salts, which were dissolved in deionized water.

Cell culture

HL-7702 and SMMC-7721 cells were cultured in DMEM and RPMI 1640 medium, respectively, supplemented with 10 % fetal bovine serum (Invitrogen), 1 % penicillin, and 1 % streptomycin. The cells were seeded in confocal culture dishes and then incubated for 24 h at 37 °C under a humidified atmosphere containing 5 % CO_2.

Cell imaging

The cells were detached and replanted on glass-bottomed dishes before HL-7702 cells and SMMC-7721 cells imaging. For monitoring of viscosity in living cells, cells were exposed to OA (5.0 μM, 30 min); then, cells were treated with PV-1 (5.0 μM, 30 min) before being washed three times with PBS. For the control assay, cells were treated with PV-1 (5.0 μM, 30 min). To study PV-1 specically targeted in peroxisomes, First, cells were stained with Peroxisome-GFP (3.0 μL, 10^8 particle·ml^{-1}, 28 h), then treated with PV-1 (5.0 μM, 30 min) after being induced with OA (5.0 μM, 30 min). The time-dependent fluorescence imaging of the HL-7702 cells incubated with OA (5.0 μM) for 30 min, then treated with PV-1 (5.0 μM) for 30 min. The HL-7702 cells have good intact shape before they are imaged. The cell images were recorded on a Leica TCS SP8 microscope with a 63x oil-immersion objective (N/A 1.3).

Mouse models and in vivo liver imaging

The C57 mice (female, 5 weeks old, 16 -18 g) were purchased from the laboratory animal center of Shandong University (Jinan, China).For monitoring in vivo livers viscosity in mice with non-alcohol Fatty Liver disease. C57 mice were randomly divided into three groups, control group, experimental group and treatment group. For the experimental group and scavenging group, the mice were treated with high-fat forage (60 kcal% Fat) for six weeks. And treatment group the mice were treated with the same dose N-acetyl cysteine (NAC, 10 mg/kg), votamins E (8 mg/kg) and pioglitazone (4 mg/kg) by intragastric administration every two days. The mice were performed imaging after were intravenously injected with PV-1 (100 μL, 10^{-4} M) for 30 min. The C57 mice were fasted for 12 h to avoid possible food fluorescence interference to the dye fluorescence before imaging.

Statistical analysis

The data were accumulated from at least three independent experiments in same condition. All data are expressed as the mean ± S.D. For each experiment, unless otherwise noted, n represents the number of individual biological replicates, n = 3.

For cell imaging, we first randomly selected three images. Then, we selected the three ROIs in one image to calculate average fluorescence intensity. To normalize the fluorescence intensity of images, the average fluorescence intensity of the control group referenced as "1". The fluorescence intensity of other groups compared with the control group to obtain relative fluorescence intensity of (b) and (c) in revised manuscript.

For in vivo imaging, we first collected the average fluorescence intensity and PA intensity of the whole spectrum in three experiments. Then, to normalize the fluorescence intensity of images, the average fluorescence intensity of the control group referenced as "1". The fluorescence intensity of other groups compared with the control group to obtain relative fluorescence intensity experimental group and scavenger group.

Fluorescence quantum yield

We choose cresyl violet acetates, which has a fluorescence quantum yield of 0.54 in ethanol, as the reference. According to the following standard equation (1), the quantum yield of PV-1 determined in mixed aqueous (glycerol-methanol), respectively.

$$\varphi_1 = \frac{\varphi_B I_1}{I_B}\frac{A_B}{A_1}\frac{\lambda_{exB}}{\lambda_{ex1}}\frac{\eta_1}{\eta_B}$$

φ : quantum yield; I : integrated area under the uncorrected emission spectra; A : absorbance at the excitation wavelength; λ_{ex} : the excitation wavelength; η : the refractive index of the solution.

The Förster-Hoffmann equation

The Förster-Hoffmann equation was utilized to correlate the relationship between the fluorescence emission intensity of the PV-1 and the solvent viscosity.

$$\log I = C + x \log \eta$$

in which η is the viscosity, I is the fluorescence emission or photoacoustic intensity, C is a constant and x represents the sensitivity of the fluorescent probe to the viscosity.

Furthermore, Förster–Hoffmann equation was utilized to correlate the relationship between the fluorescence lifetime (log τ) and viscosity (log η).

$$\log \tau = C + x \log \eta$$

in which η is the viscosity, τ is the fluorescence lifetime, C is a constant and x represents the sensitivity of the fluorescent probe to the viscosity.

Synthesis of probe PV-1

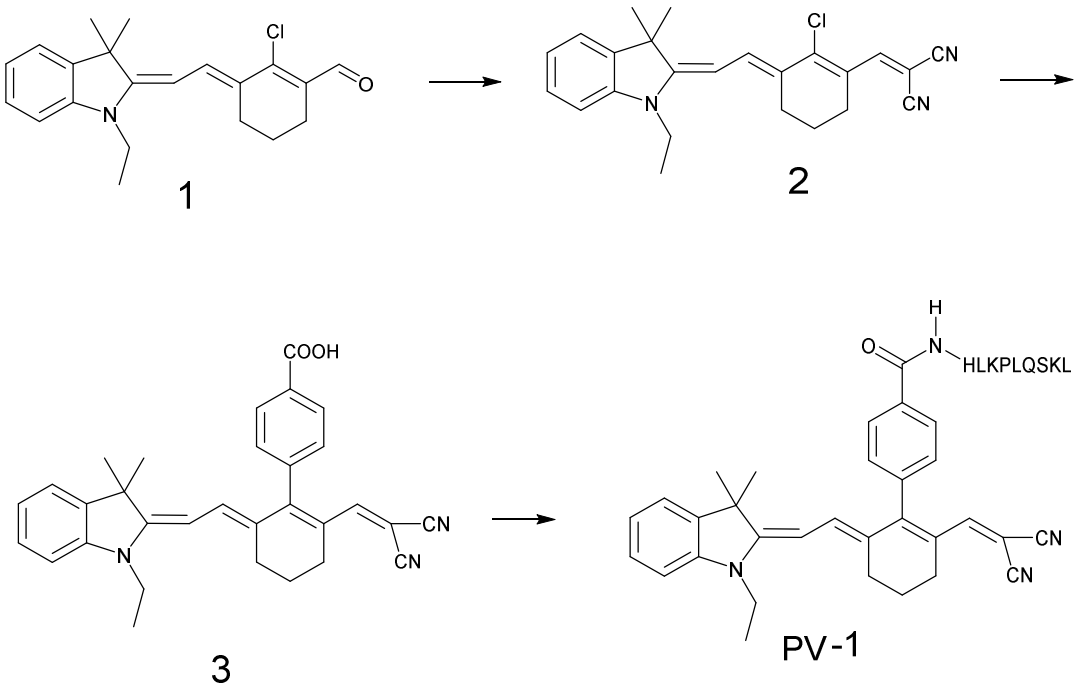

This new peroxisomal-targeting fluorescent probe PV-1 was synthesized according to the above steps. Compound 1 was prepared according to the previous literature. The synthesis of compound 2 and 3 were described below.

Synthesis of compound 2: To a methanol solution containing compound 2 (59 mg, 0.15 mmol) and malononitrile (99 mg, 1.5 mmol), saturated K_2CO_3 methanol solution (4.0 mL) was added. The solution was stirred at room temperature until the starting materials disappeared. The solvent in the collected filtrate was evaporated, and the product was purified by silica gel column chromatography (CH_2Cl_2) as a blue crystal was obtained and was filtered to give compound 2(12 mg, 20%). ^{1}H NMR ($CHCl_3$, 400 MHz) δ 7.92 (d, 20 Hz, 2H), 7.34 (d, J = 7.2 Hz, 2H), 7.21 (t, J = 3.6 Hz, 1H), 7.00 (t, J = 7.6 Hz, 1H), 6.78 (d, J = 8.0 Hz, 1H), 5.59 (d, J = 13.2 Hz, 2 H), 3.32 (m, 2H), 2.85 (t, J = 6 Hz, 2H), 2.50 (t, J = 6 Hz, 2H), 1.81 (m, 2H), 1.61 (s, 6H), 0.83 (t, J = 6.0 Hz, 3H). 13C NMR (DMSO, 100 MHz) δ 166.32, 152.50, 147.29, 141.90, 138.86, 136.74, 127.25, 123.80, 122.49, 121.67, 120.78, 128.59, 116.47, 114.74, 106.80, 93.85, 46.62, 36.70, 28.68, 26.45, 24.90, 21.78, 19.94. HRMS(ESI): calculated for $C_{24}H_{24}ClN_3$, $[M+H]^+$ = 389.1659, found 390.1727.

Synthesis of Compound 3: The mixture of compounds 2 (0.1 mmol, 39mg), 4-Carboxyphenylboronic acid (0.2 mmol, 33mg) $K_3PO_4 \cdot 3H_2O$ (0.1 mmol, 33.8 mg), Pd $(PPh_3)_4$ (0.01 mmol, 11.6 mg) dissolved in 3 mL DMF/H_2O (v/v = 5:1). Then, the reaction solution was stirred at 90 °C for 5h. After that, the solvent was cooled to room temperature, then 100 mL ice water was added, the mixture was extracted three times with CH_2Cl_2. The organic phase was separated, washed with brine, and dried

with anhydrous Na_2SO_4. The solvent in the collected filtrate was evaporated, and the product was purified by silica gel column chromatography (CH_2Cl_2/MeOH = 10: 1, v/v) to give the pure compound 3 as a blue solid (12mg, 26%). ^{1}H NMR (DMSO, 400 MHz) δ 8.08 (d, 12 Hz, 2H), 7.34 (d, J = 7.2 Hz, 1H), 7.26 (d, J = 8.0 Hz, 2H), 7.23 (d, J = 7.6 Hz, 1H),7.07 (d, J = 8.0 Hz, 1H), 6.98 (t, J = 7.6 Hz, 1H), 6.62 (d, J = 13.2 Hz, 1H), 6.57 (s, 1H), 5.83 (d, J = 12 Hz, 1H), 3.94 (d, J = 6.4 Hz, 2H), 2.79 (t, J = 5.6 Hz, 2H), 2.58 (t, J = 5.2 Hz, 2H), 2.00 (m, 2H). 1.00 (s, 6H), 0.85 (t, J = 6.4 Hz, 3H). 13C NMR (DMSO, 100 MHz) δ 175.12, 166.10, 159.99, 154.53, 147.24, 143.16, 142.76, 142.38, 139.32, 130.26, 130.11, 129.60, 128.59, 126.66, 122.85, 122.64, 118.70, 117.17, 109.27, 47.29, 34.67, 29.64, 29.20, 27,12, 25.66, 22.28. HRMS(ESI): calculated for $C_{31}H_{29}N_3O_2$, $[M-H]^-$=474.1180, found 474.2204.

PV-1 was provided by Sangon Biotech. HRMS(ESI): Theoretical calculated for $C_{80}H_{113}N_{17}O_{13}$, [M] = 1520.516, $[M+2H]^{2+}$ = 761.258, $[M+3H]^{3+}$ = 508.172, found [M] = 1521.00, $[M+2H]^{2+}$ = 761.15, $[M+3H]^{3+}$ = 508.00, respectively.

The final structures of compound 2 and 3 were well-characterized with ^{1}HNMR, ^{13}C NMR, and high-resolution mass spectrometry (HRMS). PV-1 was well-characterized with HRMS and HPLC.

Table S1 Test viscosity, λ_{abc}/nm, λ_{em}/nm , $\xi^c/M^{-1}cm^{-1}$ and fluorescence quantum yield (***φ%***) of PV-1 (5.0 μM) in the varied of the methanol/glycerol (v/v) mixtures at 29.7 ℃.

Glycerol/methanol (v:v)	η/cp	λ_{abc}/nm	λ_{em}/nm	$\xi^c/M^{-1}cm^{-1}$	*φ*/%
0:10	2	645	695	40000	0.7
1:9	12	650	695	47000	0.8
2:8	23	654	698	47100	1.3
3:7	33	659	700	47400	1.6
4:6	47	660	700	50400	1.9
5:5	54	660	700	52500	2.6
6:4	64	660	700	57200	2.9
7:3	86	660	701	57800	3.8
7.5:2.5	113	662	702	62500	4.3
8:2	143	665	703	66300	4.5
8.5:1.5	222	666	703	70300	7.0
9:1	271	667	704	70600	9.0
9.5:0.5	463	668	705	71200	11.0
10:0	643	670	706	72600	13.0

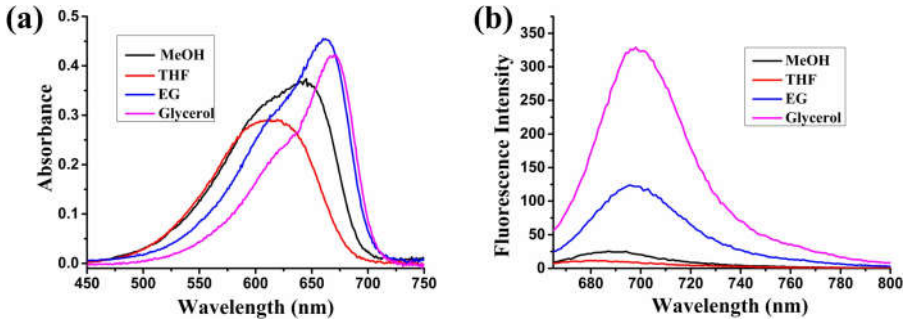

Fig. S1 UV spectra (a) and fluorescence spectra (b) of PV-1 (5.0 μM) in different solvents, respectively. MeOH (0.60 cp, ε=55.4), THF (0.53 cp, ε=37.4), EG (30.0 cp, ε=56.3), glycerol (643 cp, ε=57.0). λ_{ex} = 650 nm.

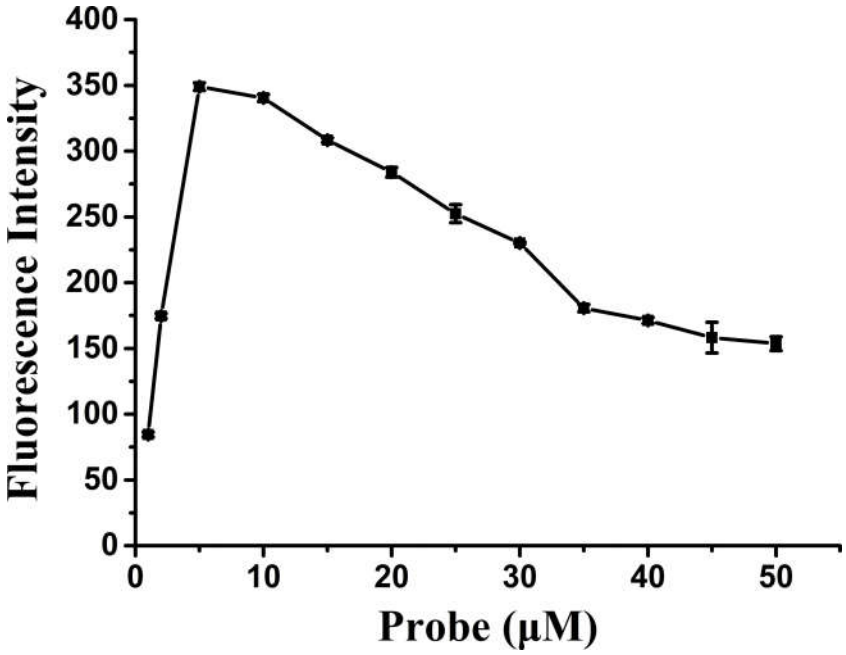

Fig. S2 The optimization of PV-1 concentration. λ_{ex} = 650 nm, λ_{em} = 705 nm.

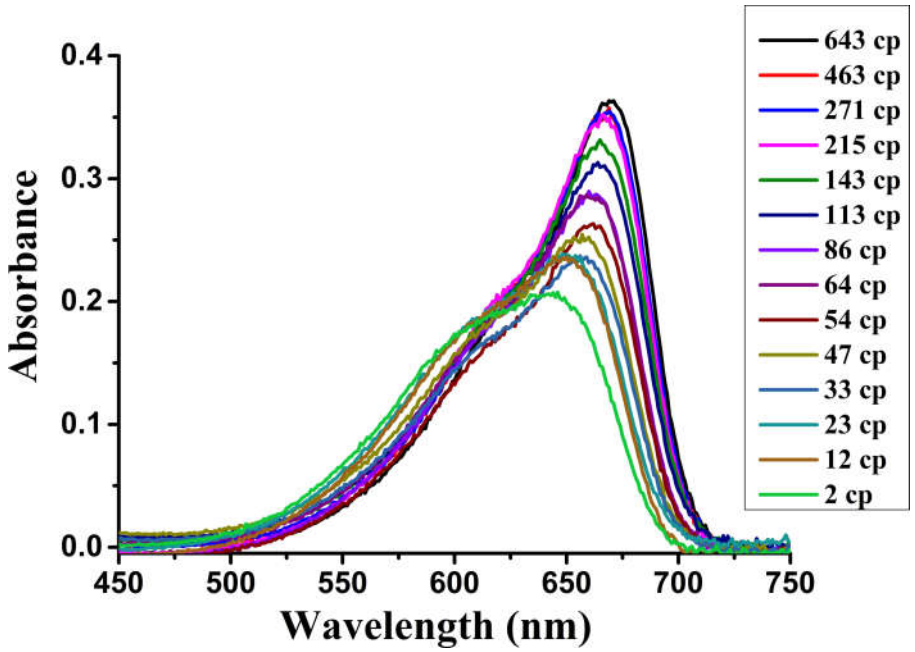

Fig. S3 The fit curves of the Absorption spectra of PV-1 in methanol-glycerol solvent systems.

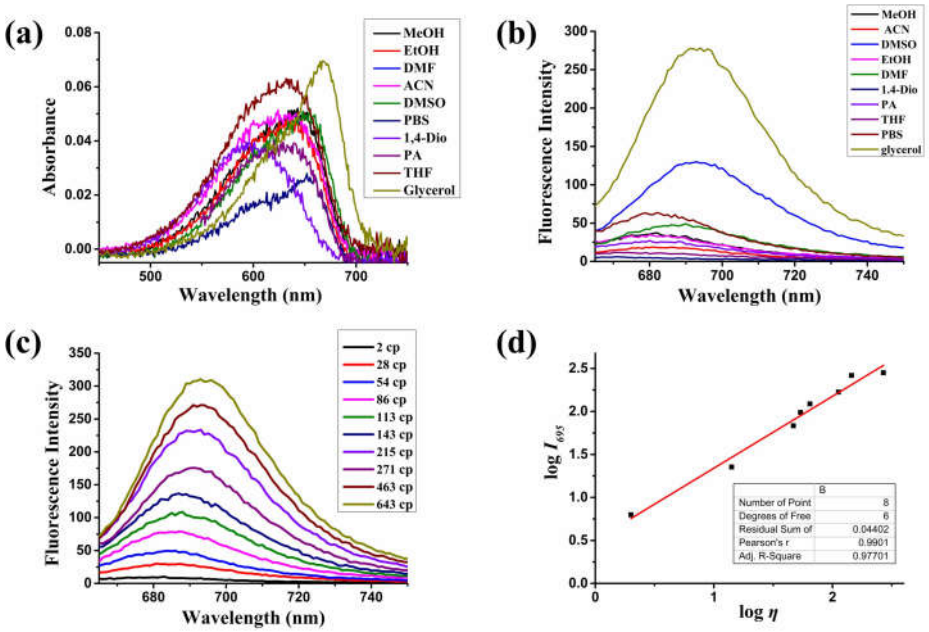

Fig. S4 UV spectra **(a)** and fluorescence spectra **(b)** of probe precursor 3 (5.0 μM) in different solvents, respectively. Fluorescence spectra **(c)** and linear relationship **(d)** of probe precursor 3 (5.0 μM) in different methol-glycerol systems. λ_{ex} = 650 nm, λ_{em} = 695 nm.

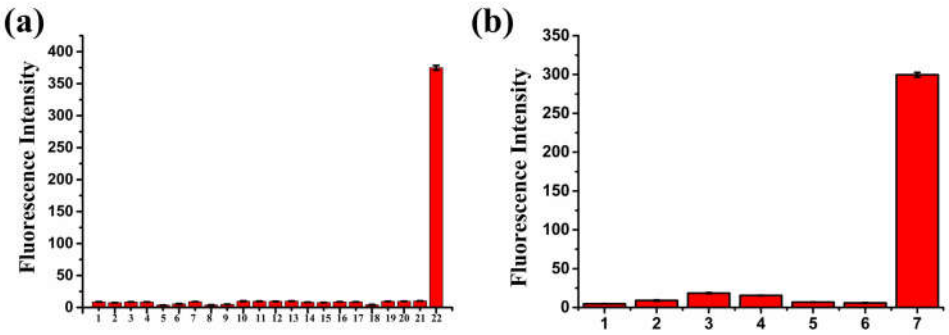

Fig. S5 The selectivity of the PV-1. **(a)** The fluorescence intensities of PV-1 (5.0 μM) to various relevant analytes in phosphate buffer (PBS, 10 mM, pH = 8.2). 1: K^+ (5 mM); 2: Na^+ (5 mM); 3: H_2O_2 (1 mM); 4: Ca^{2+} (200 μM); 5:Mg^{2+} (200 μM); 6: Zn^{2+} (200 μM); 7: Fe^{2+} (200 μM); 8: Fe^{3+} (200 μM); 9: Cu^{2+} (200 μM); 10: Al^{3+}(200 μM) 11: GSH (100 μM); 12: Hcy (100 μM); 13: Cys (200 μM); 14: ClO^- (10 μM); 15: $^{\cdot}OH$ (10 μM); 16: NO (10 μM); 17: HS^- (10 μM); 18: TBHP (10 μM); 19: $ONOO^-$(10 μM); 20: $O_2^{\cdot-}$(10 μM) 21: blank; 22: glycerol (99%). **(b)** The fluorescence intensities of PV-1 (5.0 μM) to different proteins in phosphate buffer. 1: blank; 2: Esterase (1.0 KU/L); 3. BSA (20 μM); 4: ALP (200.0 KU/L); 5: AChE (5.0 KU/L); 6: DNase (5.0 KU/L); 7: glycerol (99%). λ_{ex}= 650 nm, λ_{em} = 705 nm.

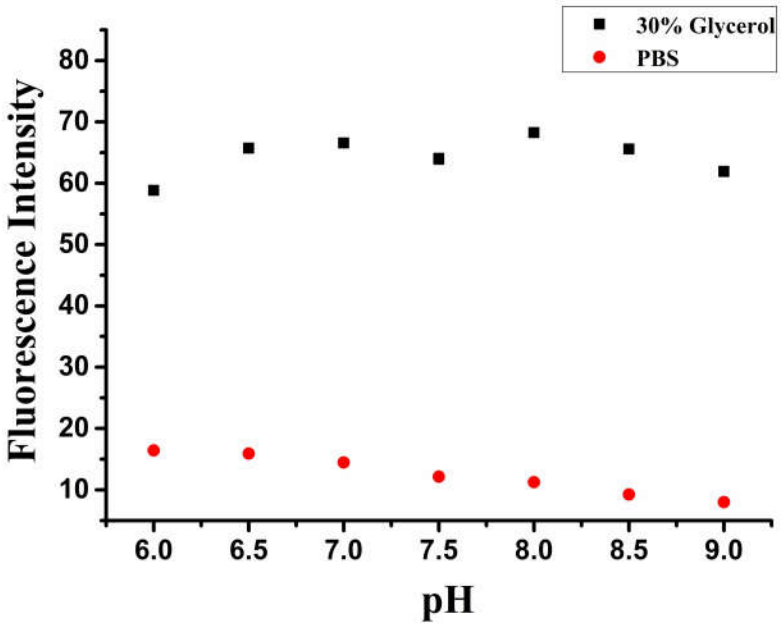

Fig. S6 The pH effects on the PV-1. The fluorescence intensity of PV-1 (5.0 μM) under different pH values (6.0 - 9.0). As above data, PV-1 responded well under 30 % glycerol. λ_{ex} = 650 nm, λ_{em} = 705 nm.

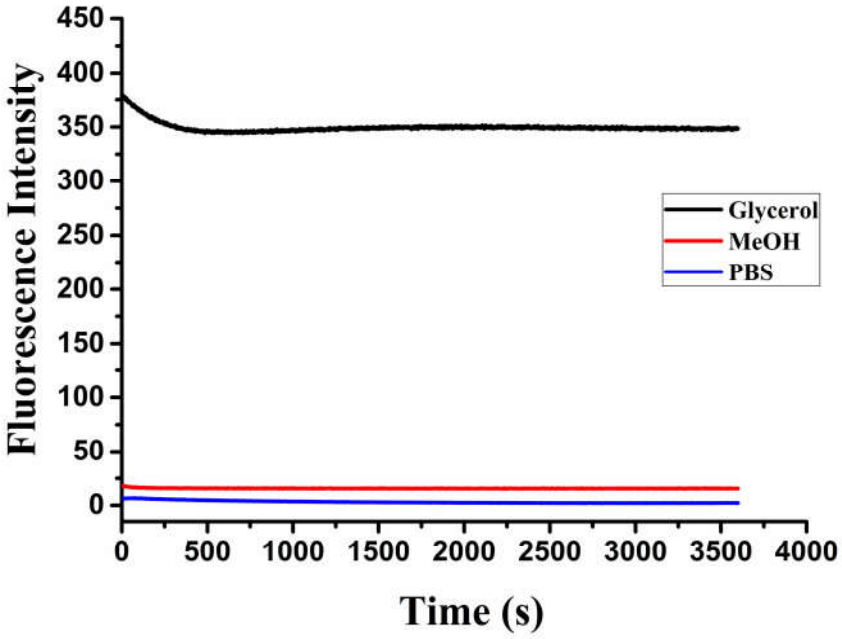

Fig. S7 The Photo-stability experiments of PV-1 (5.0 μM) under MeOH, PBS (pH = 8.2, 10.0 mM) and glycerol condition by laser light for 60 min. λ_{ex} = 650 nm, λ_{em} = 705 nm.

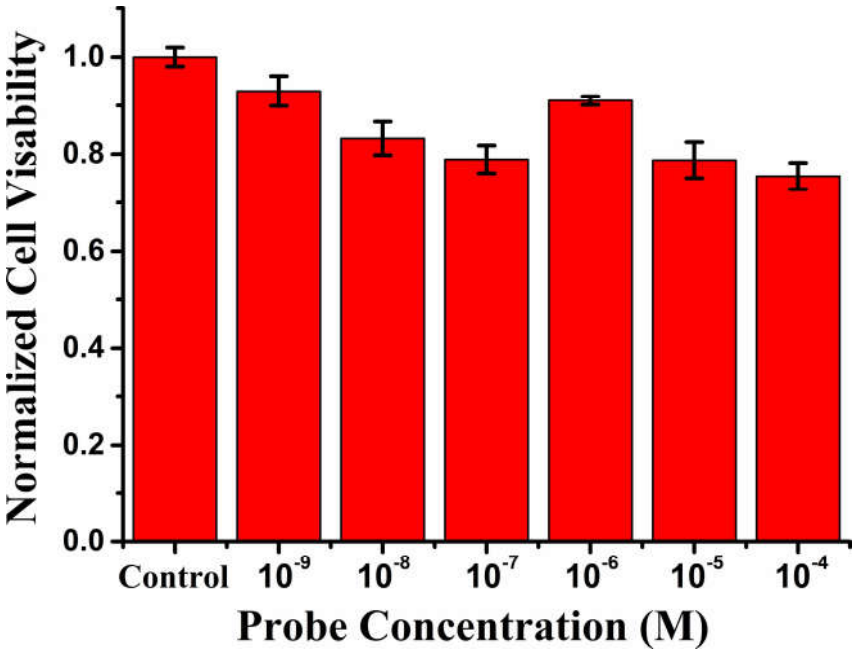

Fig. S8 The MTT assay of HL-7702 cells in different concentrations of PV-1.

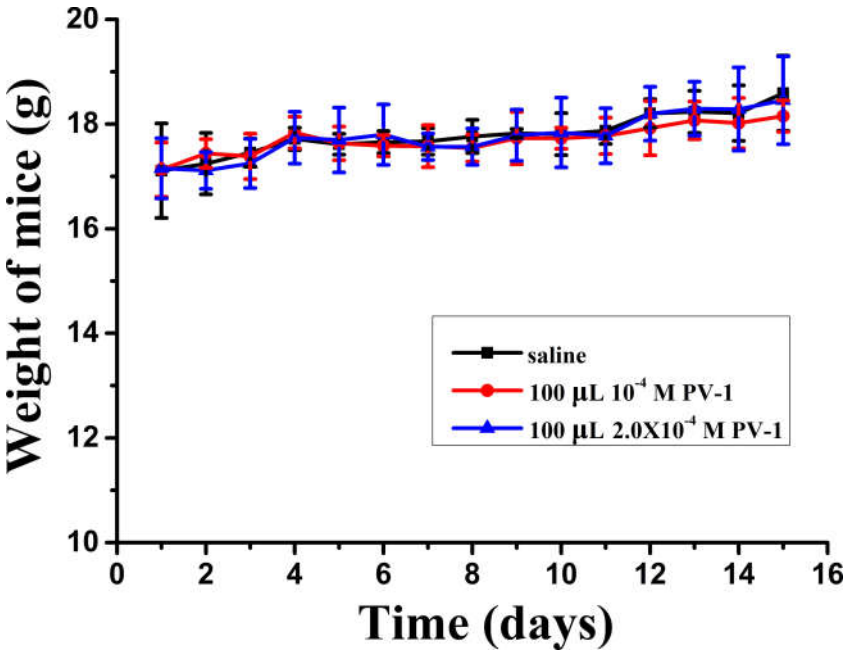

Fig. S9 In vivo toxicity of PV-1 in C57 mice. C57 mice were randomly divided into three groups, control group, experimental group. Experimental group were treated with different PV-1 (100 µL, 10^{-4} M and 200 µL, 10^{-4} M) by intragastric administration. The control group were treated with 100 µL saline. The weight changes of mice in the experimental group were compared with control group for two weeks. The results showed that the body weight of mice in the experimental group were basically as the same as that of the control group. Moreover, the mice in the experimental group didn't show any disease symptoms such as hair loss, scarring and vomiting. Therefore, PV-1 exhibits low cytotoxicity in vivo. n = 5.

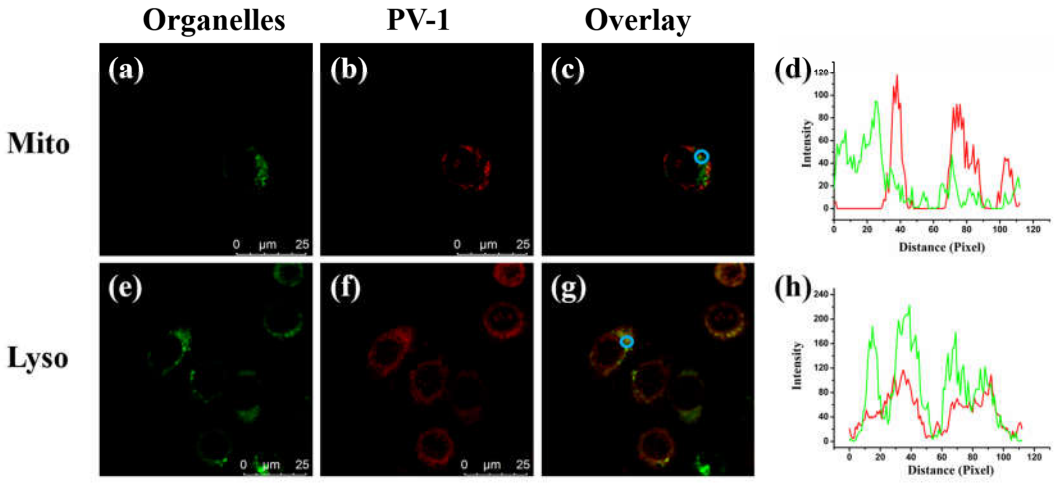

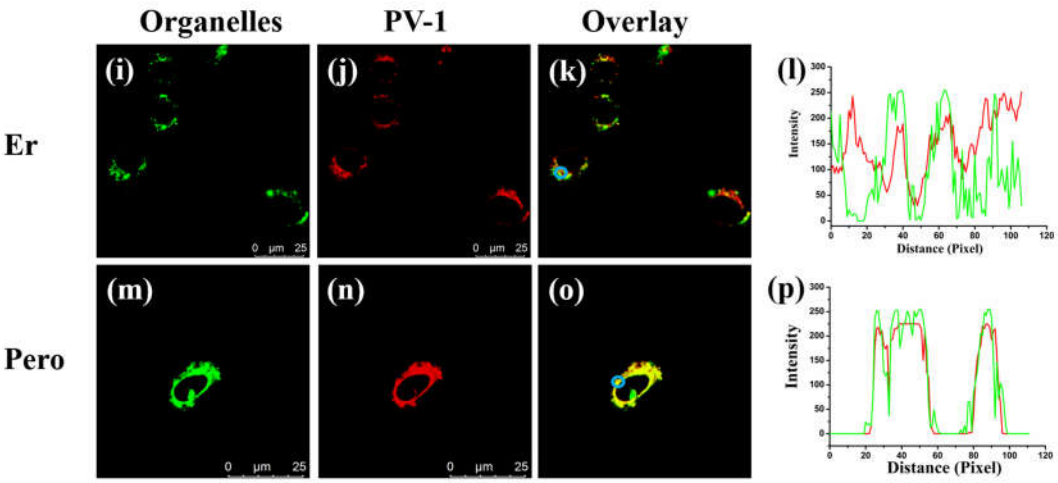

Fig. S10 Co-localization fluorescence images of HL-7702 cells stained with PV-1 and commercial dyes. First, HL-7702 cells were stained with OA (5.0 μM, 0.5 h), then treated with PV-1 (5.0 μM) and organelle dyes for 30.0 min, including, mito-Tracker green (100 nM, λ_{ex} = 488 nm, λ_{em} = 500 – 550 nm), Lyso-Tracker green (100 nM, λ_{ex} = 488 nm, λ_{em} = 500 – 550 nm). ER-Tracker Red (50 nM, λ_{ex} = 561 nm, λ_{em} = 580 – 630 nm), Peroxisome-GFP (3.0 μL, 10^8 particle·ml^{-1}, 28 h, λ_{ex} = 488 nm, λ_{em} = 500 – 550 nm). The co-localization coefficient was about 0.31, 0.47 and 0.31 for mitochondria, lysosomes and endoplasmic reticulum, respectively. So, PV-1 exhibited the poor co-localization with other organelles. PV-1 (λ_{ex} = 633 nm, λ_{em} = 650 – 750 nm), Scale bar: 25 μm.

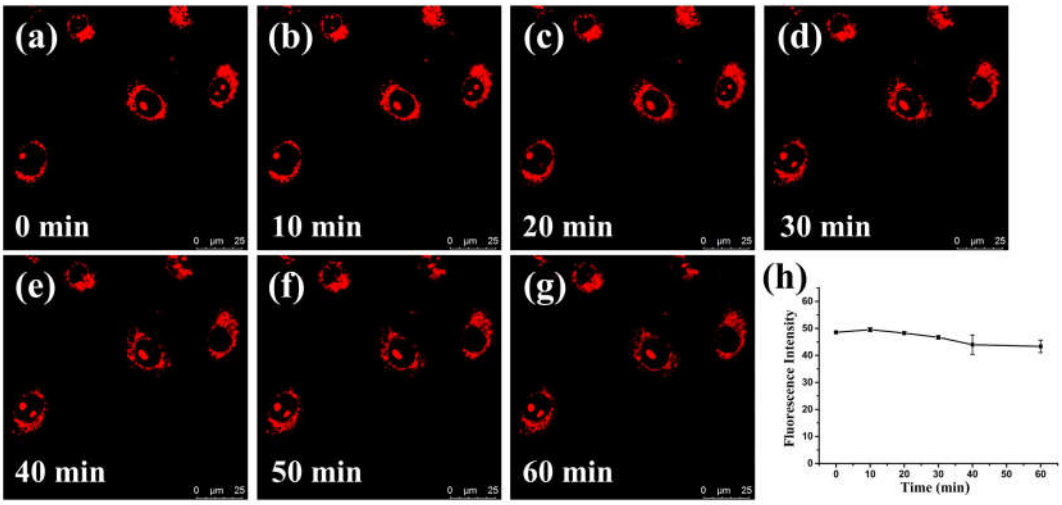

Fig. S11 Time-dependent fluorescence imaging of PV-1. Fluorescence images of HL-7702 cells stained with PV-1 (5.0 μM, 30.0 min) and other organelles after being induced with OA (5.0 μM, 30.0 min). PV-1 (λ_{ex} = 633 nm, λ_{em} = 650 – 750 nm), Scale bar: 25 μm.

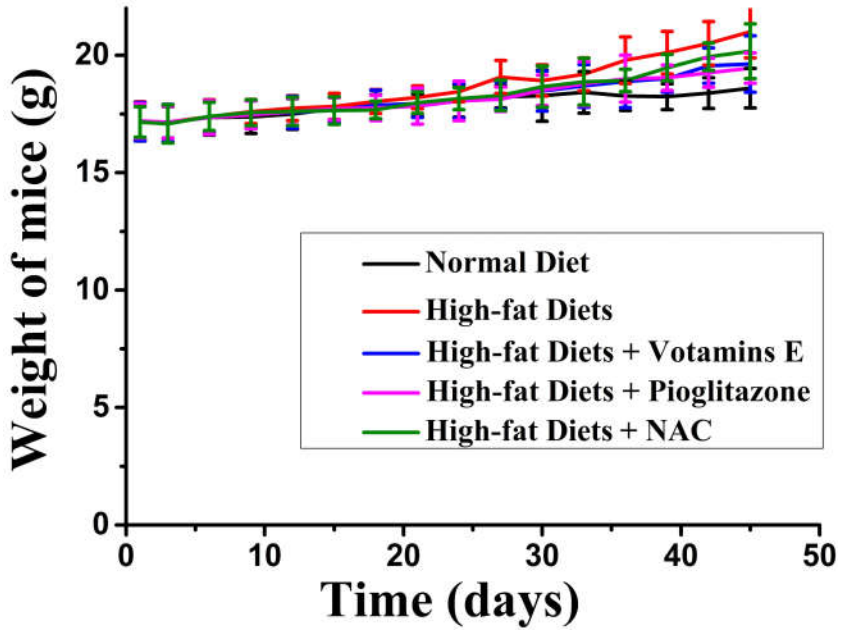

Fig. S12 Weight of normal mice and mice with NAFLD for six weeks. Animal weights were monitored every three days for the three groups. C57 mice were randomly divided into three groups, control group, experimental group and treatment group. Experimental group were treated with high-fat diet every day. Treatment group were with high-fat diet (60 kcal % Fat) and NAC (10 mg/kg), vitamins E (8 mg/kg), pioglitazone (4 mg/kg) every two days. The control group were treated with normal diet. n = 10.

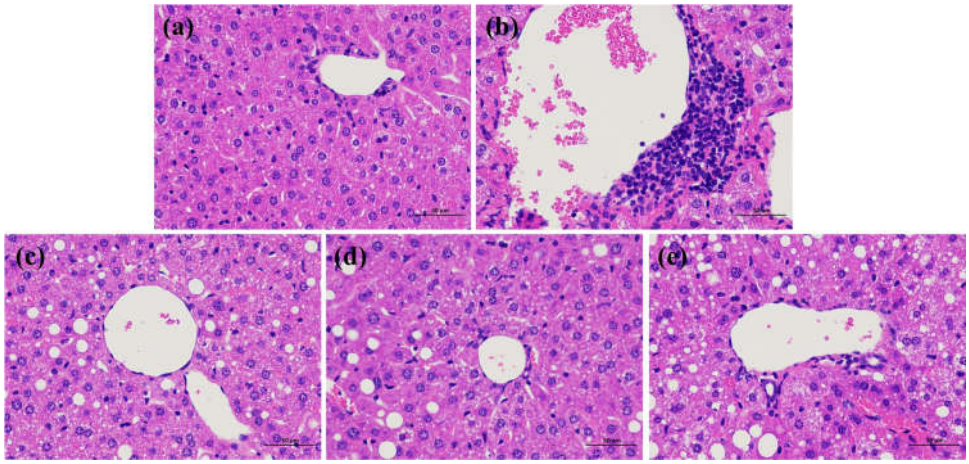

Fig. S13 Hematoxylin and eosin (H&E) staining of mice's livers. (a) Normal liver tissue. The hepatic lobule structure was clear, the hepatic cords were arranged neatly, no obvious expansion or extrusion of hepatic sinus and inflammation. (b) Liver tissue of NAFLD. There are some symptoms, such as large areas of hepatocyte steatosis, lymphocytic foci, and collagen hyperplasia. (c) Liver tissue of NAFLD + vitamins E, (d) Liver tissue of NAFLD + pioglitazone and (e) Liver tissue of NAFLD + NAC. There are large amounts of hepatocyte steatosis, and circular vacuoles and lymphocytic infiltration, and bile duct hyperplasia. Scale bar = 50 μm.

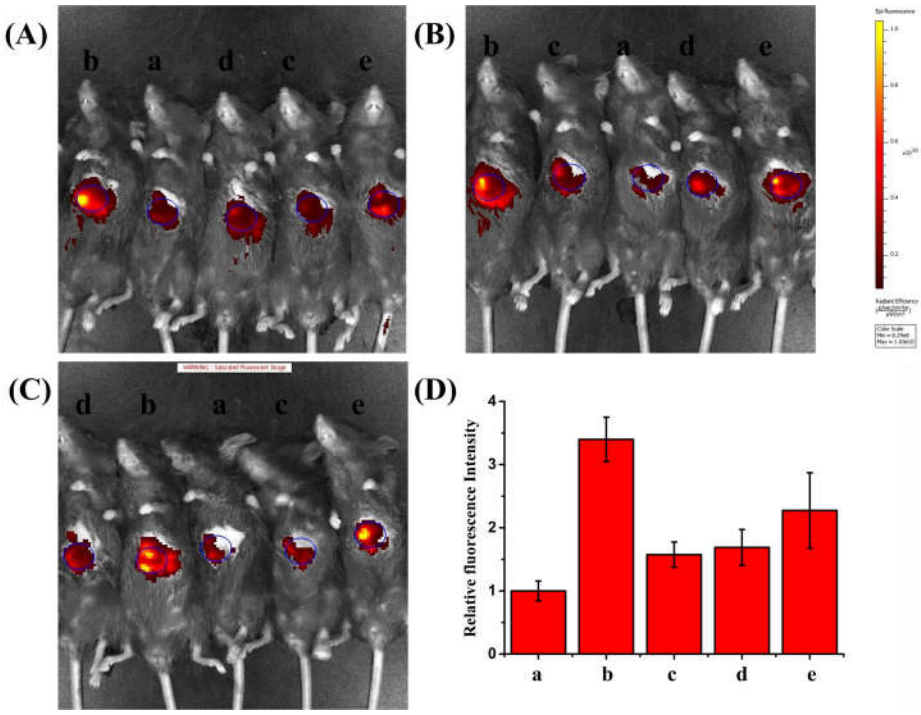

Fig. S14 (A)(B)(C) Fluorescence images of the mouse's liver after the injection of PV-1 for 30 min. we randomize the positions of the animals. a: Normal mice. b: NAFLD mice. c: NAFLD mice + vitamins E. d: NAFLD mice + pioglitazone. e: NAFLD mice + NAC. The blue circle is roughly the liver (D) Relative fluorescence intensity to the normal mice. n = 3. λ_{ex} = 660 nm, λ_{em} = 710 nm.

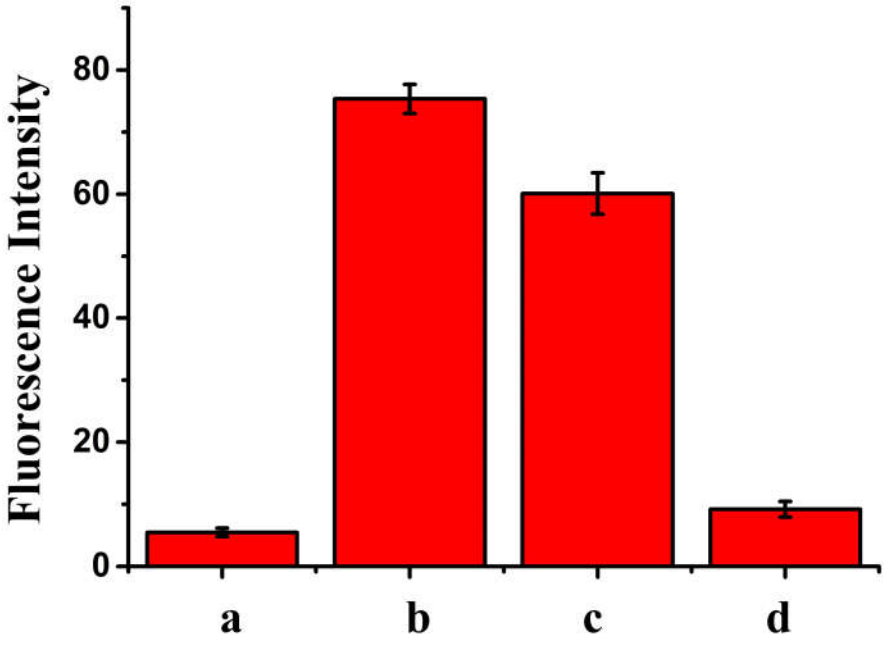

Fig. S15 Fluorescence intensity of PV-1 in fresh liver tissue homogenate supernatant under NAC condition. a: PBS (pH = 7.4); b: fresh liver tissue homogenate supernatant + PV-1(5.0 μM); c: fresh liver tissue homogenate supernatant + NAC + PV-1(5.0 μM); d: PBS + NAC + PV-1(5.0 μM). λ_{ex} = 650 nm, λ_{em} = 705 nm. n = 5.

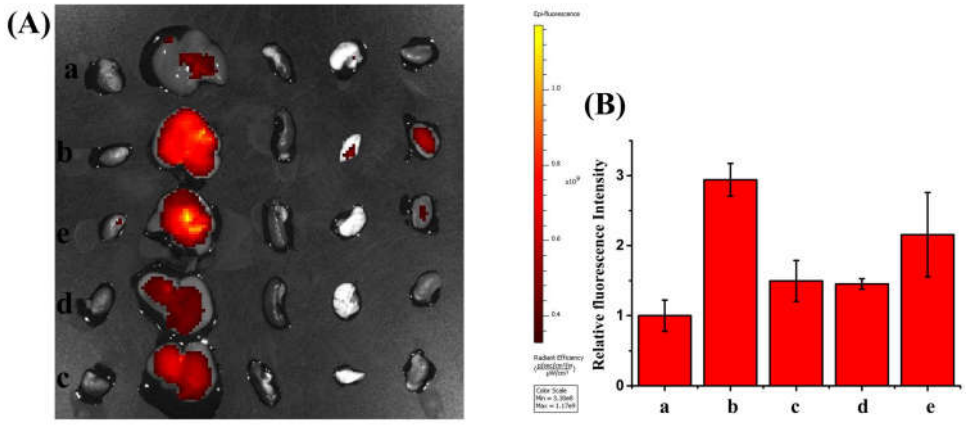

Fig. S16 (A) Fluorescence images of the different organs (heart, liver, spleen, lung and kidney) after the injection of PV-1 for 30 min. a: Normal liver tissue. b: Liver tissue of NAFLD. c: Liver tissue of NAFLD + vitamins E. d: Liver tissue of NAFLD + pioglitazone. e: Liver tissue of NAFLD + NAC. (B) Relative fluorescence intensity to the normal mice. The values are the mean ± s.d. for n = 3. λ_{ex} = 660 nm, λ_{em} = 710 nm.

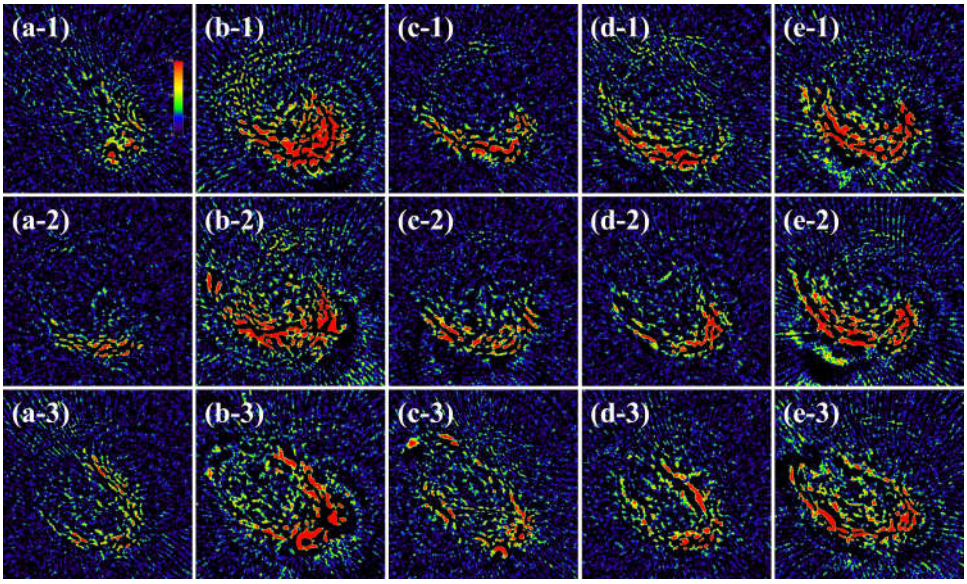

Fig. S17 $PA_{680\ nm}$ images of the mouse's liver after the injection of PV-1 for 30 min. (a-1,2,3) Normal mice. (b-1,2,3) NAFLD mice + PV-1. (c-1,2,3) NAFLD mice + vitamins E + PV-1. (d-1,2,3) NAFLD mice + pioglitazone+ PV-1. (e-1,2,3) NAFLD mice + NAC+ PV-1. n = 3.

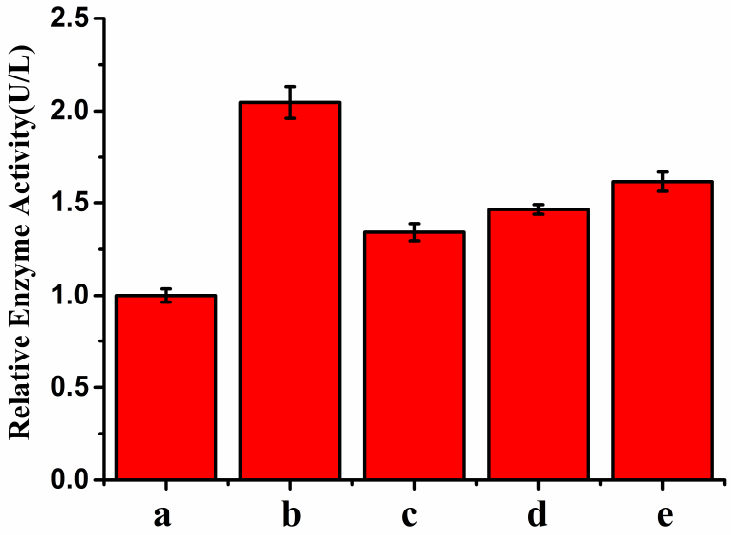

Fig. S18 The relative alanine aminotransferase (ALT) content in mice liver. a: Normal liver tissue. b: Liver tissue of NAFLD. c: Liver tissue of NAFLD + vitamins E. d: Liver tissue of NAFLD + pioglitazone. e: Liver tissue of NAFLD + NAC. The values are the mean ± s.d. for n = 5.

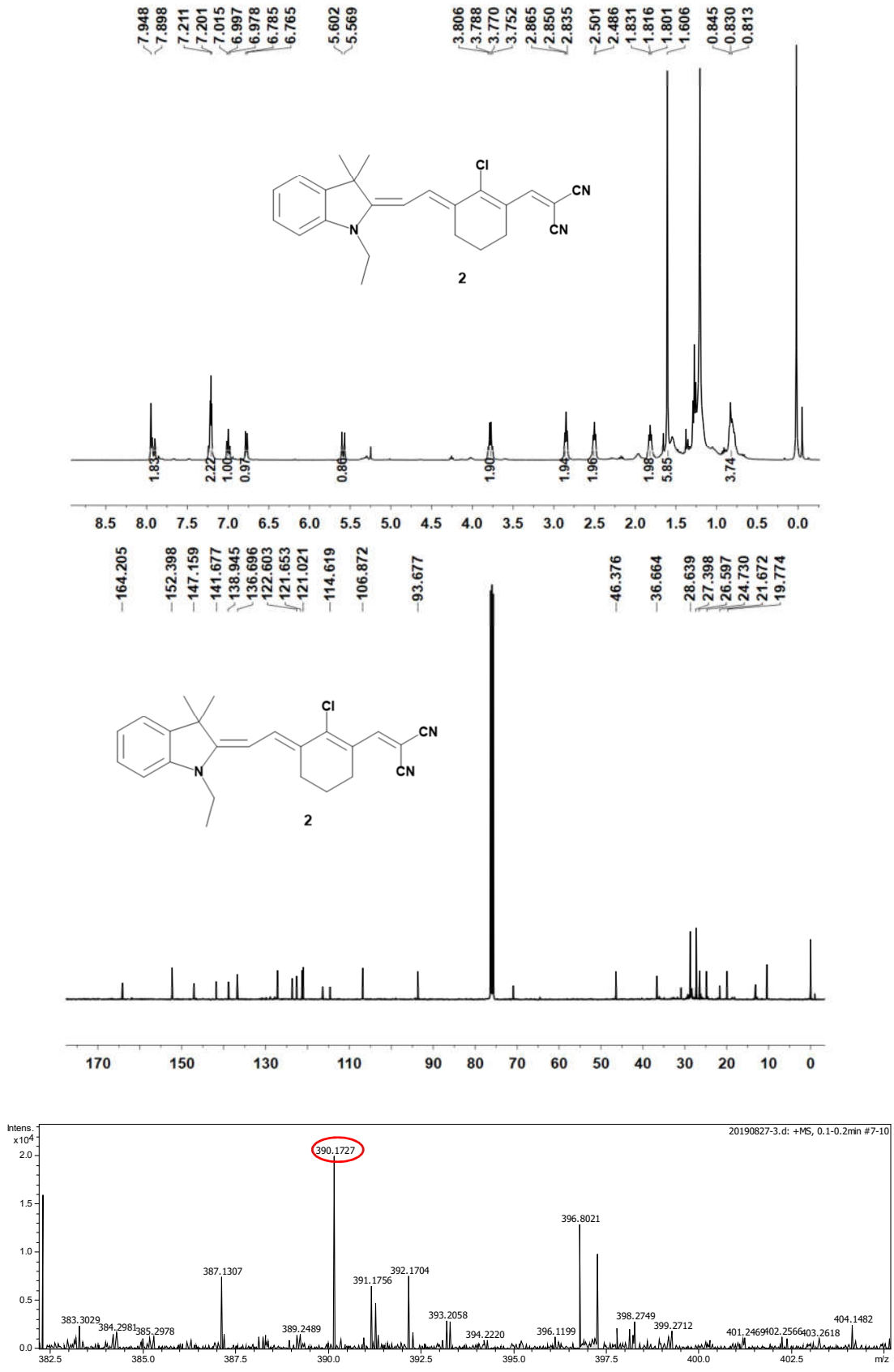

Fig. S19 The ^{1}H NMR, ^{13}C NMR and HRMS data of compound 2.

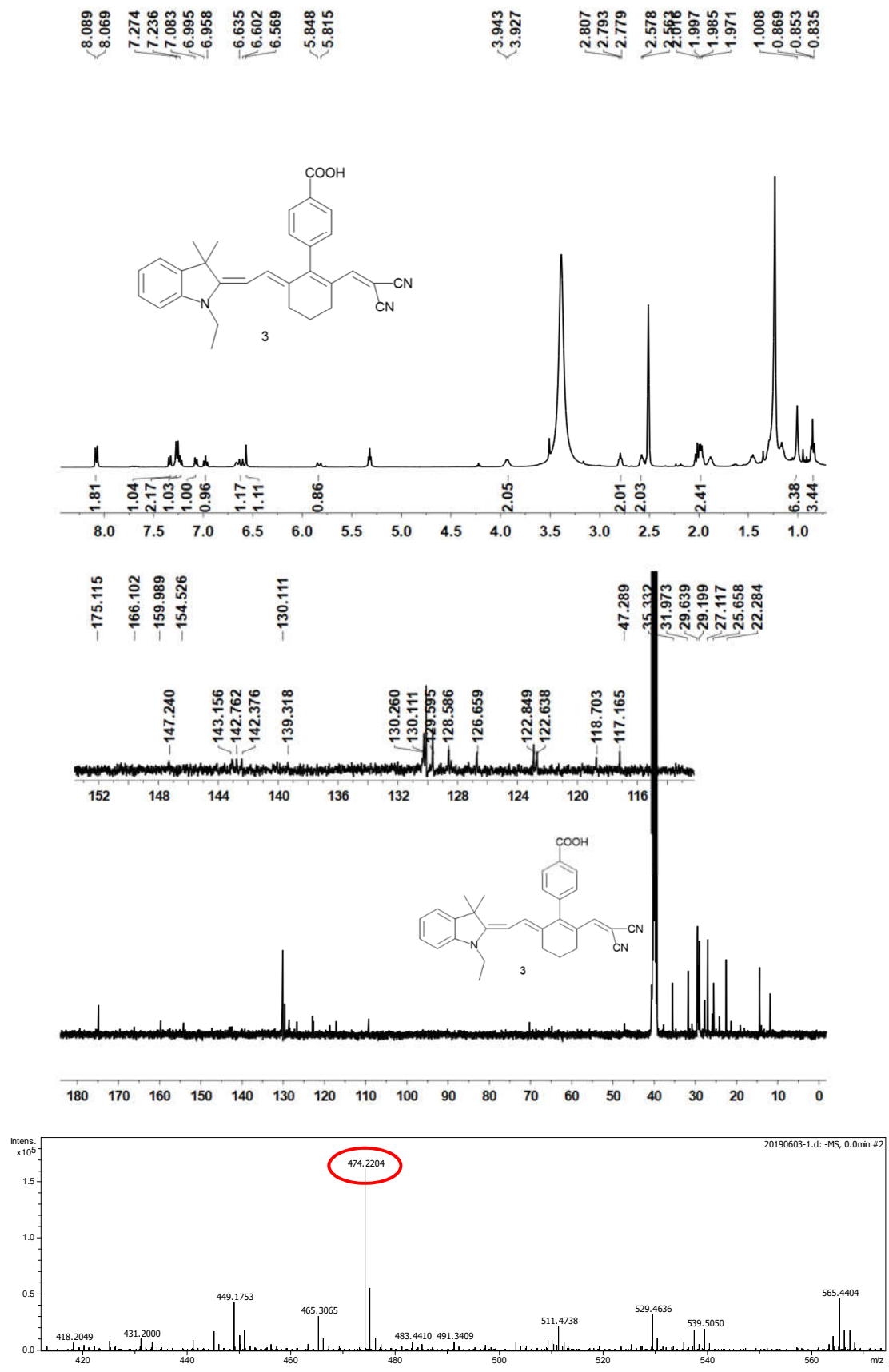

Fig. S20 The ^{1}H NMR, ^{13}C NMR and HRMS data of compound 3.

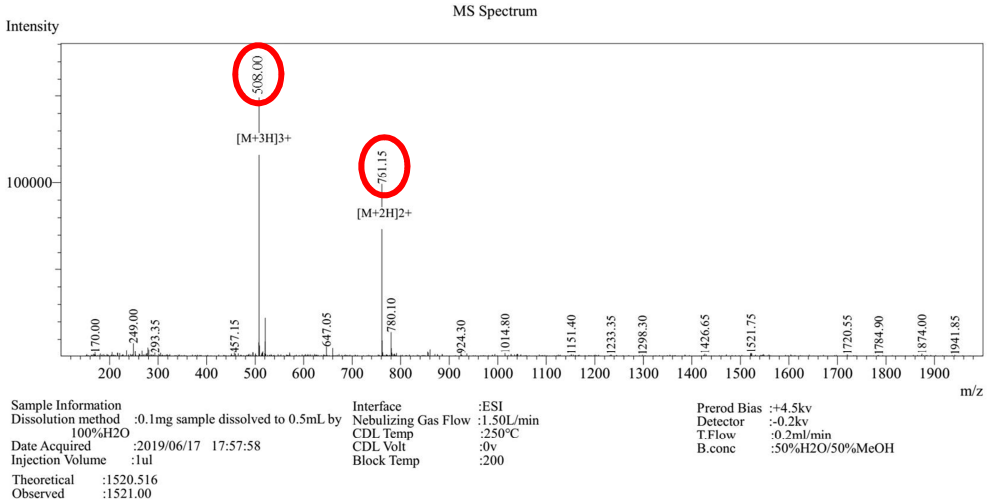

Pump A	:	0.1%trifluoroacetic in 100%water
Pump B	:	0.1%trifluoroacetic in 100%acetonrtrile
Total Flow	:	1.0ml/min
Wavelength	:	214nm
Analytical column type	:	SHIMADZU Inertsil ODS-SP(4.6*250MM*5UM)
Dissolution method	:	0.5mg sample dissolved to 0.5mL by 100%H2O
Acquisition Time	:	2019/06/17 16:41:52
Inj.Volume	:	60ul

Time	Module	Action	Value
0.01	Pumps	B.Conc	33
20.00	Pumps	B.Conc	53
20.01	Pumps	B.Conc	95
27.01	Pumps	B.Conc	95
27.02	Controller	Stop	

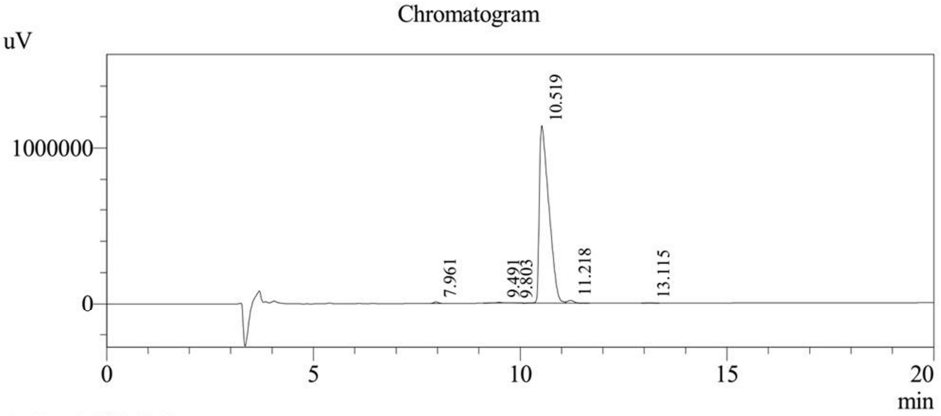

1 Det.A Ch1 / 214nm

PeakTable

Detector A Ch1 214nm

Peak#	Ret. Time	Area	Height	Area %	Height %
1	7.961	72268	10104	0.391	0.862
2	9.491	57883	4249	0.313	0.363
3	9.803	20508	1349	0.111	0.115
4	10.519	18135580	1136936	98.033	97.053
5	11.218	191667	16804	1.036	1.434
6	13.115	21559	2014	0.117	0.172
Total		18499464	1171455	100.000	100.000

Fig. S21 The MS and HPLC data of probe PV-1.